# Canine Prostate: Contrast-enhanced US-guided Radiofrequency Ablation with Urethral and Neurovascular Cooling—Initial Experience[1]

Ji-Bin Liu, MD
Gervais Wansaicheong, MBBS
Daniel A. Merton, BS, RDMS
See-Ying Chiou, MD
Yao Sun, MD
Kai Li, MD
Flemming Forsberg, PhD
Pamela R. Edmonds, MD
Laurence Needleman, MD
Ethan J. Halpern, MD

**Purpose:** To prospectively evaluate in a canine model contrast material–enhanced ultrasonography (US) for guiding and monitoring radiofrequency (RF) ablation of the entire prostate, with urethral and vascular cooling to protect the surrounding structures.

**Materials and Methods:** After approval by the institutional animal use and care committee, an RF electrode was used to ablate the entire prostate in 15 dogs. During ablation, pulse-inversion harmonic US was performed by using an endocavitary probe after an intravenous bolus injection (0.04 mL/kg) and infusion (0.015 μL/kg/min) of a US contrast agent. In group 1 ($n = 4$), no cooling protection was used during ablation. In group 2 ($n = 5$), urethral and bladder protection was provided by inserting a 12-F catheter infused with cold saline (8°C ± 4 [standard deviation]) at a rate of 100 mL/min. In group 3 ($n = 6$), further protection of the neurovascular bundles (NVBs) was provided by infusing cold saline (8°C ± 4) into the iliac arteries at a rate of 50 mL/min by means of catheterization of the femoral artery. Pathologic findings among the three groups were compared by using the Wilcoxon rank sum test.

**Results:** The average volumes of prostate ablation achieved in the three groups were 96.6%, 91.9%, and 92%. Contrast-enhanced pulse-inversion harmonic US allowed visualization and monitoring of urethral and NVB blood flow during the ablation. Without protection, damage to the urethra and the NVB was demonstrated at both US and pathologic examination. There was highly significant difference in urethral damage between groups with and the group without urethral cooling ($P = .002$), while intraarterial cooling demonstrated a nonsignificant trend toward a decreased NVB damage ($P = .069$).

**Conclusion:** Contrast-enhanced US can guide RF ablation of the entire prostate. Infusion of cold saline provides effective protection for the urethra during such procedures. The application of intraarterial cooling did not provide a significant improvement in the protection of the NVB in this small study.



[1] From the Department of Radiology, Thomas Jefferson University, 7th Floor Main Building, 132 S 10th St, Philadelphia, PA 19107 (J.B.L., D.A.M., F.F., P.R.E., L.N., E.J.H.); Department of Diagnostic Radiology, Tan Tock Seng Hospital, Singapore (G.W.); Department of Radiology, Taipei Veterans General Hospital, Taipei, Taiwan (S.Y.C.); Shandong Provincial Medical Imaging Research Institute, Shandong, China (Y.S.); and Department of Ultrasound, Third Hospital of Sun Yat-Sen University, Guangzhou, China (K.L.). Received July 27, 2007; revision requested September 26; revision received October 4; final version accepted December 10. Supported in part by National Institutes of Health grant EB002794. **Address correspondence to** J.B.L. (e-mail: *ji-bin.liu@jefferson.edu*).

Pathologic specimens from radical prostatectomies demonstrate that prostate cancer is multifocal in 85% of patients (1–4). Given the multifocal nature of prostate cancer, treatment of localized prostate cancer requires destruction of the entire gland. Radiation therapy and radical prostatectomy are effective treatments, but are associated with substantial morbidity (1–5). To minimize the complications of therapy for prostate cancer, several alternative treatments for localized prostate cancer have emerged (6). During the past 2 decades, the use of brachytherapy for the treatment of prostate cancer has increased markedly (7). More recently, several minimally invasive therapies have been investigated for an in situ treatment of prostate cancer, including cryosurgical ablation (8), interstitial laser therapy (9), high-intensity focused ultrasound (10), and microwave coagulation (11). These procedures are performed transperineally, transurethrally, or transrectally. The common goal of these therapies is the destruction of the entire prostate and the tumor tissue within.

Radiofrequency (RF) thermal ablation has been used experimentally and clinically for the treatment of hepatic and other tumors (12). A major challenge to clinical use of RF therapy is the inability to distinguish viable tissue and tumor from necrotic tissue during ablation. Lack of such definition may lead to overtreatment or undertreatment. Although ultrasonography (US) is used for guiding needle placement, conventional gray-scale and Doppler imaging cannot reliably depict residual viable tissue and tumor.

Our preliminary animal study has demonstrated that contrast material–enhanced US imaging can be used to guide and monitor RF ablation of the entire prostate gland (13). To minimize the possibility of injury to the adjacent structures during the ablation of the entire prostate and to avoid damage to critical structures, including the urethra and bladder and neurovascular bundles (NVBs), protective methods need to be explored. Thus, the objective of our current study was to prospectively evaluate in a canine model contrast-enhanced US for guiding and monitoring RF ablation of the entire prostate, with urethral and vascular cooling to protect the surrounding structures.

### Advances in Knowledge

- The feasibility of contrast-enhanced US for guiding and monitoring radiofrequency thermal ablation of the entire prostate in a canine model has been demonstrated.
- Cooling techniques for protecting the urethra and the neurovascular bundles during radiofrequency ablation have been developed and tested.

### Implication for Patient Care

- Radiofrequency thermal ablation of the entire prostate guided with contrast-enhanced US may provide a minimally invasive method for an alternative treatment of prostate cancer.

## Materials and Methods

The animal protocol used in this project was approved by our institutional animal use and care committee, and all husbandry and experimental studies were compliant with the National Institutes of Health Guide for Care and Use of Laboratory Animals (*http://oacu.od.nih.gov/regs/guide/guidex.htm*). This study was supported in part by GE Healthcare, Oslo, Norway, who provided the lipid-based US contrast agent, Sonazoid. The authors of this article had sole control of the data generated by this study and the information provided for publication.

### RF Ablation System

An RF generator (Cool-tip; Valleylab, Boulder, Colo) was used for prostate ablation. A single electrode with a 1- or 2-cm exposed RF tip was used to deliver the RF energy. The 17-gauge electrode is internally cooled with 4°–8°C water circulated by a hydraulic pump. To complete the electrical circuit, a standard grounding pad was affixed to a well-shaved back of the subject.

### US Contrast Agent and Imaging Protocols

The contrast agent Sonazoid (GE Healthcare, Oslo, Norway) consists of encapsulated microbubbles of a perfluorobutane gas with a mean diameter of 3 μm. Transrectal US examination was performed by using an Elegra (Siemens Medical Solutions, Issaquah, Wash) scanner. An endocavitary probe (6.5EC10; Siemens Medical Solutions) along with a needle-guide attachment was used to guide insertion of the electrode. Gray-scale pulse-inversion harmonic mode was used with a transmission frequency of 2.8 MHz (ie, receiving at 5.6 MHz) during intravenous bolus injection (0.04 mL/kg) and infusion (0.015 μL/kg/min) of the contrast agent. The mechanical index was kept below 0.4 to minimize microbubble destruction. Contrast-enhanced imaging of the prostate in each dog was achieved with a bolus injection of the contrast agent before RF ablation, continuous infusion during the RF ablation, and a follow-up bolus injection after completion of the ablation.

### Animal Model

Fifteen adult male mongrel dogs (weight, 20–33 kg) were divided into three groups. Prior to the experiments, the animals were anesthetized with 2%–4%

**Published online before print**
10.1148/radiol.2473071334

**Radiology 2008;** 247:717–725

**Abbreviations:**
NVB = neurovascular bundle
RF = radiofrequency
TTC = triphenyltetrazolium chloride

**Author contributions:**
Guarantor of integrity of entire study, J.B.L.; study concepts/study design or data acquisition or data analysis/interpretation, all authors; manuscript drafting or manuscript revision for important intellectual content, all authors; approval of final version of submitted manuscript, all authors; literature research, J.B.L., G.W., S.Y.C., K.L.; experimental studies, J.B.L., G.W., D.A.M., S.Y.C., Y.S., K.L., F.F., P.R.E., L.N.; statistical analysis, F.F., E.J.H.; and manuscript editing, all authors

See Materials and Methods for pertinent disclosures.

isoflurane via an endotracheal tube. Cardiac and respiratory parameters were monitored throughout the procedures. An intravenous fluid channel was established through an 18-gauge angiographic catheter placed in a forelimb vein for contrast material injection.

In group 1, four dogs were studied to demonstrate whole prostate ablation with contrast-enhanced US guidance. In our previous experiments (13), we noticed that the increased periurethral blood flow due to hyperemia seemed to act as a natural heat sink. We hypothesize that this may protect the urethra during thermal ablation of the prostate gland. Therefore, no additional protective cooling measure was taken for group 1 dogs to validate our hypothesis.

In group 2, five dogs were studied to demonstrate whole prostate ablation with the addition of protective cooling of the urethra. Cooling of the urethra and bladder was achieved by means of catheterization of the urinary bladder with a 12-F three-way Foley catheter and continuous circulation of cold saline by using a hydraulic pump (Valleylab) to provide continuous cooling at the flow rate of 100 mL/min. The temperature of the circulated saline from a 500-mL bottle was maintained at 8°C ± 4 (standard deviation) and was monitored with a thermometer. To achieve the desired saline temperature, the bottle of saline was placed in an ice-filled container and the temperature was adjusted by adding 250–500 mL of alcohol to the ice container. The added alcohol absorbs the heat from the saline and lowers the saline temperature rapidly. Use of saline for urethral cooling should not affect conductivity of the RF ablation, since the saline does not enter the prostate tissue.

In group 3, six dogs were studied to demonstrate whole prostate ablation with additional protective cooling of the urethra and the NVBs. Cooling of the NVB was achieved by means of catheterization of the iliac artery with a 6-F angiographic catheter. The insertion procedure was performed with a femoral artery puncture and US guidance. The catheter was advanced to the aortic bifurcation and the catheter tip was visualized with conventional US imaging. Confirmation of the position was performed with an injection of a small amount of the US contrast agent, when necessary. The catheter, located at the aortic bifurcation, was infused with cold saline (8°C ± 4) at a flow rate of 50 mL/min when the area of ablation approached 1 cm from the NVBs.

### Imaging and Ablation Protocol

On baseline transrectal gray-scale images, the prostate volume was calculated by means of measurements made transversely and sagittally in the anteroposterior, transverse, and cephalocaudal dimensions by using an ellipsoid formula (D.A.M., J.B.L., in consensus, both with 23 years of US imaging experience). Transverse images were also acquired throughout the prostate at 5-mm intervals, starting from the base to the apex before and after ablation. These images were recorded on the hard drive of the US unit and S-VHS videotapes for later analysis.

RF ablation of the entire prostate was performed sequentially in the *(a)* mid gland, *(b)* base, *(c)* apex, and *(d)* contrast-enhanced residual viable areas of the gland. On the basis of our previous findings, RF ablation of the targeted region was achieved during 5–12 minutes by using power settings of 5–30 W (13). These ablation parameters were adjusted so that a larger area of ablation was achieved in the mid portion of the gland and a smaller area was produced at the base and apex of the gland. Ablations were performed by using an electrode with a 2-cm tip; however, an electrode with a 1-cm exposed tip was used for precise targeted ablation of small residual areas of enhancing (ie, viable) tissue to more completely ablate the entire prostate. After each RF ablation, a sufficient interval (10–15 minutes) was allowed for cooling of the ablated site before contrast-enhanced imaging was performed to assess the ablation area. The end point of the procedure was determined according to findings of contrast-enhanced imaging, that is, ablation was continued until all intraparenchymal enhancement was gone.

The presence of perfused (ie, contrast-enhanced) periurethral tissue and a persistent flow in the NVBs were assessed visually at real-time pulse-inversion harmonic US. This was performed during infusion and after bolus injection of the contrast agent (J.B.L., D.A.M., in consensus). A semi-quantitative assessment of the residual viable tissue was obtained (J.B.L. and S.Y.C. in consensus; S.Y.C. had 10 years of US imaging experience) from the postablation contrast-enhanced US sections by using digital imaging analysis software (ImageJ; National Institutes of Health, Bethesda, Md). The imaging volume was calculated by adding the cross-sectional area on each section and multiplying it by the section thickness (5 mm).

### Pathologic Assessment

After the RF ablation procedure, the animals were sacrificed with intravenous injection of 100 mg/kg sodium pentobarbital (Euthasol; Virbac AH, Fort Worth, Tex). The entire prostate was excised and serially sliced by using a custom-made gantry slicer. The specimen was precisely sliced at equidistant 5-mm intervals beginning at the apex and continuing to the base of the prostate (ie, corresponding to the transverse images obtained in vivo). A thorough gross inspection of the surrounding structures, including urethra, urinary bladder, and rectum, was performed (J.B.L.) to evaluate for injury or burns.

After slicing was completed, an assay with triphenyltetrazolium chloride (TTC) was performed to determine tissue viability (14). This made it easier to distinguish small residual viable prostatic tissue from coagulative tissue. By using a 1% TTC solution with pH 7.8 at room temperature, viable tissue stained dark purple-red while nonviable tissue remained pale. After 90 minutes of TTC incubation, the slices were digitally photographed alongside a ruler for later measurements. The volume of each prostate was calculated by adding the cross-sectional area of the prostate on each specimen slice and multiplying it by the slice thicknesses (5 mm). The irregularly shaped residual viable areas of the TTC-stained specimens were

measured in the same manner as the US measurements by using software (J.B.L.). The total prostate ablation volume was calculated for each prostate as the total prostate volume minus the total volume of residual viable tissue.

Finally, all prostate slices were fixed in 10% formalin and embedded in paraffin blocks. The blocks were sectioned with a whole-mount method and stained with standard hematoxylin-eosin stain for light microscopic assessment by a pathologist (P.R.E., with 7-year prostate pathology experience). By using both TTC- and hematoxylin-eosin–stained specimens, the urethra was divided into quadrants and each quadrant was scored as positive or negative (ie, completely normal tissues) for the presence of thermal damage. Individual quadrant scores were combined to determine an overall score corresponding to the percentage of damage in each urethra (ie, 0, 0.25, 0.50, 0.75, or 1.0). Microscopic evaluation of serial whole-mount slides was used to assess damage of the NVBs. For each NVB, if the microscopic structures of the nerve and adjacent vessels of the NVB region were damaged, the thermal damage was scored as positive. The thermal damage scores for the two NVBs in each dog were combined into an overall NVB damage score for each dog (ie, 0, 0.5, or 1.0).

### Statistical Analysis

Since this was a pilot study, we had no prior estimate of the expected variance in our outcome measurement. The sample size for each group was set to five in order to obtain preliminary data for future studies. Because of technical difficulties, one animal was lost from group 1 and an additional dog was included in group 3. All measured volumes were expressed as the mean (in cubic centimeters) plus or minus standard deviation. The calculated prostate volumes obtained with US were compared with volumes determined from the pathologic measurements in absolute units and percentages. The calculated volumes of the residual viable tissue on contrast-enhanced US images were compared with the volumes obtained from the TTC-stained gross pathologic specimens. The percentage of the total ablation achieved was determined. A paired Student *t* test was used for statistical comparison of gland size and ablation volume between contrast-enhanced US and pathologic evaluation. A *P* value of less than .05 was considered to indicate a statistically significant difference.

Given the small sample size and our ordinal method for scoring urethral and NVB injury, the resulting data would not be expected to conform to a normal distribution. Therefore, comparison of urethral and NVB damage in the different groups was performed with the nonparametric Wilcoxon rank sum test. For urethral damage, the primary goal was to determine whether circulation of cold saline in the urethra (groups 2 and 3) prevented urethral injury (compared to group 1). An initial comparison of the degree of urethral damage was performed between groups 2 and 3 and demonstrated that there was no significant difference in urethral damage between these groups. We then proceeded to compare the degree of urethral damage between dogs without protection (group 1) and dogs with cooling protection (groups 2 and 3). With respect to NVB damage, the primary goal was to determine whether intraarterial infusion of cold saline (group 3) could prevent NVB injury (compared to groups 1 and 2). An initial comparison of the degree of NVB damage was performed between groups 1 and 2 and demonstrated that there was no significant difference in NVB damage between these groups. We then compared the degree of urethral damage between dogs without NVB protection (groups 1 and 2) and dogs with NVB protection (group 3). A *P* value of less than .05 was considered to indicate statistically significant difference. All statistical analyses were performed (F.F., E.J.H.) with software (Stata 8.0; Stata, College Station, Tex).

## Results

Transrectal US was used successfully to guide RF electrode placement with a transrectal approach in all dogs. Contrast-enhanced pulse-inversion harmonic US depicted normal prostate vasculature as a radial spoke-like pattern from the periphery to the center of the prostate, with uniform parenchymal enhancement of the entire gland. After ablation, the nonperfused area of thermal ablation appeared as a clear avascular hypoechoic defect within contrast-enhanced hyperechoic prostate parenchyma on contrast-enhanced US image (Fig 1). Although continuous intravenous infusion of contrast material was useful for real-time monitoring of the ablation, bolus injection of contrast material provided better enhancement and conspicuity between the coagulative area and the viable tissue (Figs 1, 2).

The use of contrast-enhanced pulse-inversion harmonic US facilitated identification of residual perfused areas and allowed for more precise deployment of the RF electrode (particularly for targeting small areas). The end point of the ablation was chosen to be the absence of substantial prostatic vasculature on contrast-enhanced pulse-inversion harmonic images with preservation of capsular flow. It was noted that periurethral and periprostatic blood flow increased dramatically during RF ablation, which reflects hyperemia during thermal ablation (Fig 2).

### RF Ablation of Whole Prostate

In group 1, the mean volume of the prostate was 9.99 $cm^3$ ± 5.8 (range, 1.37–13.85 $cm^3$) (Table 1). The number of ablations required for coagulation of the entire prostate ranged from four to nine (mean, 6.25) to accommodate the size differences of the prostates. There was no significant difference between the volume of residual viable tissue measured on pulse-inversion harmonic images and those measured from TTC-stained specimens (0.43 $cm^3$ ± 0.043 vs 0.41 $cm^3$ ± 0.291, $P > .21$). The average volume of prostate ablation achieved was 96.6% based on the pathologic measurements in this group (Table 1, Fig 3). In group 2, the mean volume of the prostate was 10.6 $cm^3$ ± 3.64 (range, 8.3–16.9 $cm^3$). The number of ablations required for coagulation of the entire prostate ranged from four to eight

(mean, 6.2), with an average volume of prostate ablation achieved of 91.9% (Table 2). In group 3, the mean volume of the prostate was 12.5 $cm^3$ ± 3.05 (range, 7.9–16.1 $cm^3$). The number of ablations required for coagulation of the entire prostate ranged from five to 10 (mean, 6.3). The average volume of prostate ablation achieved in group 3 was 92% (Table 3, Fig 4).

There was a statistically significant difference between the volume of the

**Figure 1**

a. b. c.

**Figure 1:** Transverse contrast-enhanced pulse-inversion harmonic US images. **(a)** Image of the prostate prior to contrast material injection. **(b)** Image shows uniform enhancement of the prostatic parenchyma with a spoke-like perfusion pattern after bolus injection (0.04 mL/kg) of contrast material. **(c)** Image after ablation of the right side of the prostate shows an avascular nonperfusion area (arrows), representing an RF-created coagulative tissue. Blood flow of the urethral wall exists and appears normal. Shadowing from urethra catheter (arrowhead) is noted.

**Figure 2**

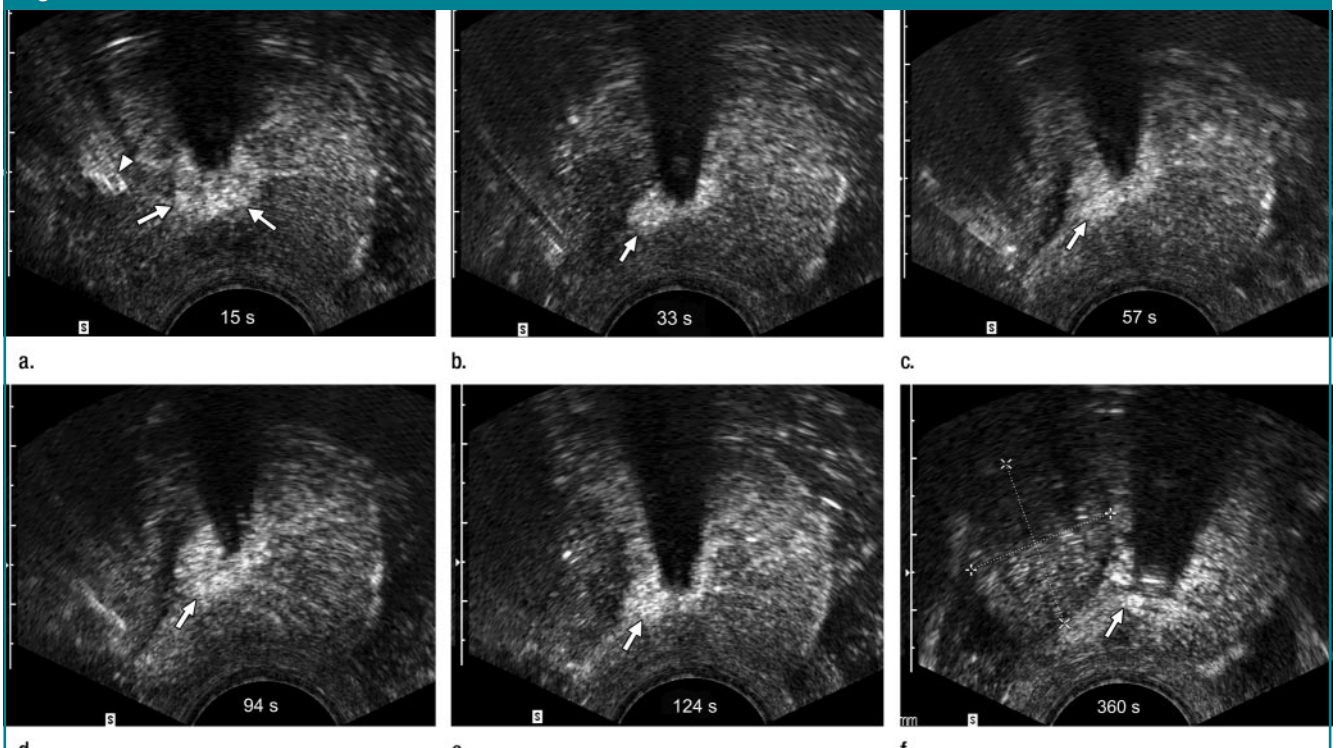


a. b. c.

d. e. f.

**Figure 2:** Sequential transverse contrast-enhanced perfusion images show the progression of the thermal coagulative tissue size on the right side of the prostate during 6 minutes of ablation at **(a)** 15, **(b)** 33, **(c)** 57, **(d)** 94, **(e)** 124, and **(f)** 360 seconds. Increasing echogenicity around the urethra is due to periurethral hyperemia (arrows). Note the artifact (arrowhead) due to RF interference from the electrode.

prostate gland measured at US and that measured at pathologic examination in absolute terms (ie, in cubic centimeters) in group 3 ($P < .001$). However, no other statistically significant differences were found in any groups with respect to comparisons of US and pathologic measurements (in absolute terms and in percentages, $P > .07$).

### RF Ablation with and without Cooling Protection

No thermal damage to the bladder or rectum was found at gross inspection. Thermal damage to the urethral wall

**Table 1**

**US and Pathologic Measurements in Group 1 ($n = 4$)**

| Dog No. | US Measurements: Prostate Volume ($cm^3$) | Viable Tissue ($cm^3$) | Ablated Tissue ($cm^3$) | Total Ablation (%)* | Pathologic Measurements: Prostate Volume ($cm^3$) | Viable Tissue ($cm^3$) | Ablated Tissue ($cm^3$) | Total Ablation (%)* |
|---|---|---|---|---|---|---|---|---|
| 1 | 12.74 | 0.33 | 12.41 | 97.41 (12.41/12.74) | 12.87 | 0.30 | 12.57 | 97.67 (12.57/12.87) |
| 2 | 11.99 | 0.76 | 11.23 | 93.66 (11.23/11.99) | 12.87 | 0.69 | 12.18 | 96.64 (12.87/12.18) |
| 3 | 13.85 | 0.14 | 13.71 | 98.99 (13.71/13.85) | 12.92 | 0.12 | 12.80 | 99.07 (12.80/12.92) |
| 4 | 1.37 | 0.12 | 1.25 | 91.24 (1.25/1.37) | 1.53 | 0.11 | 1.42 | 92.81 (1.42/1/53) |

* Data in parentheses are the numbers used to calculate the percentage.

**Figure 3**

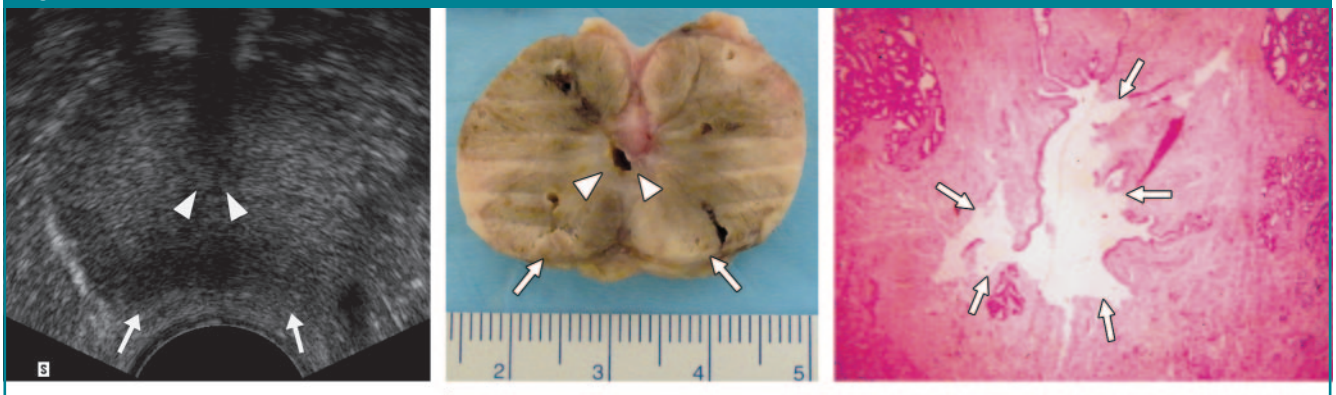


a. b. c.

**Figure 3:** **(a)** Transverse contrast-enhanced pulse-inversion harmonic US image after RF ablation in a dog without any cooling protection shows no contrast enhancement of the urethra (arrowheads) and NVB (arrows). **(b)** Gross specimen shows thermal damage of the urethral wall (arrowheads) and NVB areas (arrows). **(c)** Histologic slide shows partial damage to the urethral wall (arrows). (Hematoxylin-eosin stain; original magnification, ×10.)

**Table 2**

**US and Pathologic Measurements in Group 2 ($n = 5$)**

| Dog No. | US Measurements: Prostate Volume ($cm^3$) | Viable Tissue ($cm^3$) | Ablated Tissue ($cm^3$) | Total Ablation (%)* | Pathologic Measurements: Prostate Volume ($cm^3$) | Viable Tissue ($cm^3$) | Ablated Tissue ($cm^3$) | Total Ablation (%)* |
|---|---|---|---|---|---|---|---|---|
| 1 | 8.37 | 0.97 | 7.40 | 88.41 (7.40/8.37) | 5.76 | 0.7 | 5.06 | 87.85 (5.06/5.76) |
| 2 | 10.42 | 0.70 | 9.72 | 93.28 (9.72/10.42) | 10.65 | 1.02 | 9.63 | 90.42 (9.63/10.65) |
| 3 | 8.34 | 0.75 | 7.59 | 91.01 (7.59/8.34) | 6.25 | 0.92 | 5.33 | 85.28 (5.33/6.25) |
| 4 | 16.94 | 0.42 | 16.52 | 97.52 (16.52/16.94) | 9.73 | 0.20 | 9.53 | 97.94 (9.53/9.73) |
| 5 | 8.93 | 0.22 | 8.71 | 97.54 (8.71/8.93) | 5.95 | 0.14 | 5.81 | 97.65 (5.81/5.95) |

* Data in parentheses are the numbers used to calculate the percentage.

**Table 3**

**US and Pathologic Measurements in Group 3 ($n = 6$)**

| Dog No. | US Measurements: Prostate Volume ($cm^3$) | Viable Tissue ($cm^3$) | Ablated Tissue ($cm^3$) | Total Ablation (%)* | Pathologic Measurements: Prostate Volume ($cm^3$) | Viable Tissue ($cm^3$) | Ablated Tissue ($cm^3$) | Total Ablation (%)* |
|---|---|---|---|---|---|---|---|---|
| 1 | 13.98 | 0.86 | 13.12 | 93.85 (13.12/13,98) | 10.05 | 0.29 | 9.76 | 97.11 (9.76/10.05) |
| 2 | 9.88 | 0.65 | 6.58 | 93.42 (6.58/9.88) | 7.00 | 0.38 | 6.62 | 94.57 (6.62/7.00) |
| 3 | 7.92 | 0.56 | 7.36 | 92.93 (7.36/7.92) | 5.05 | 0.26 | 4.79 | 94.85 (4.79/5.05) |
| 4 | 14.25 | 0.43 | 13.82 | 96.98 (13.82/14.25) | 11.27 | 0.69 | 10.58 | 93.88 (10.58/11.27) |
| 5 | 16.14 | 2.46 | 13.68 | 84.76 (13.68/16.14) | 10.62 | 2.30 | 8.32 | 78.34 (8.32/10.62) |
| 6 | 12.91 | 0.73 | 12.18 | 94.35 (12.18/12.91) | 10.57 | 0.69 | 9.88 | 93.47 (9.88/10.57) |

* Data in parentheses are the numbers used to calculate the percentage.

and the NVB was demonstrated at contrast-enhanced pulse-inversion harmonic US and pathologic assessment. For the evaluation of urethral damage, there was no statistically significant difference between groups 2 and 3 (both with cooling) ($P = .14$). A highly significant difference in urethral damage was found between group 1 (without cooling) and groups 2 and 3 (both with cooling) ($P = .002$). For the assessment of NVB damage, there was no statistically significant difference between group 1 (no cooling) and group 2 (with urethral cooling only) ($P = .079$). Comparison of group 3 (with NVB cooling) with groups 1 and 2 (both without NVB cooling) failed to demonstrate a significant level of NVB protection ($P = .069$).

**Figure 4**

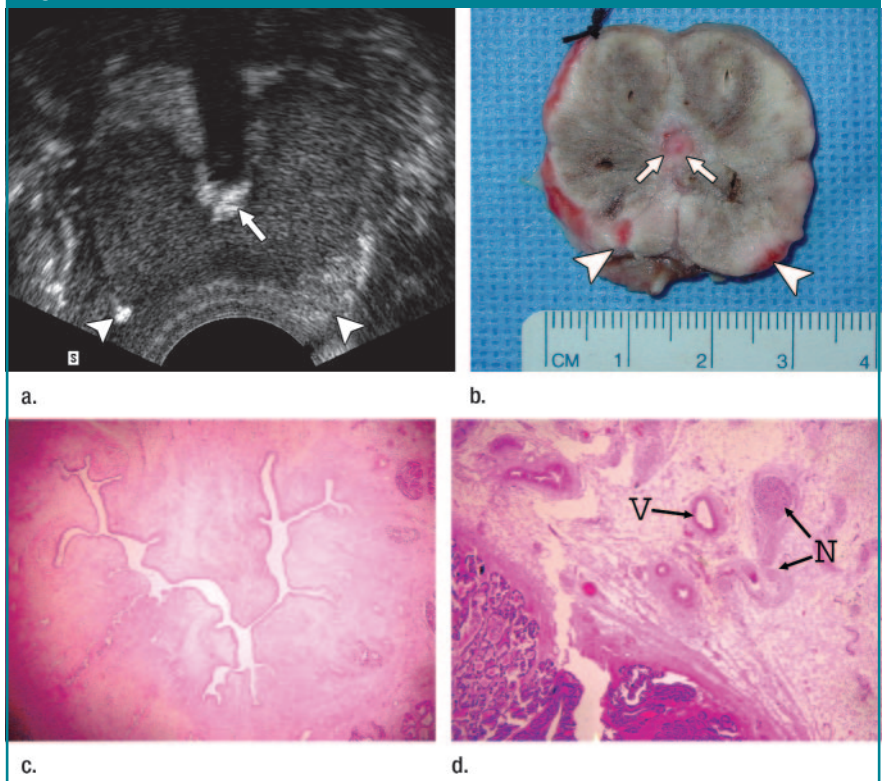


**Figure 4:** **(a)** Transverse contrast-enhanced pulse-inversion harmonic US after RF ablation demonstrates normal flow in the urethral wall (arrow) and the NVB areas (arrowheads) on both sides. **(b)** Pathologic specimen demonstrates preservation of the urethral wall (arrows) and the NVB areas (arrowheads) on both sides. Histologic slides show normal appearance of the **(c)** urethral wall and **(d)** normal NVB region ($N$ = nerve cell, $V$ = vessel). (Hematoxylin-eosin stain; magnification in **c**, ×10; magnification in **d**, ×40).

## Discussion

Because of the biologic nature of prostate cancer and the complexity of the clinical scenario, optimal management of prostate cancer remains a subject of debate. Given the high incidence of the disease and the morbidities associated with standard options, physicians and patients continue to be interested in minimally invasive treatment options. We have evaluated a therapeutic strategy for the treatment of prostate cancer in situ—RF ablation of the whole prostate guided and monitored with contrast-enhanced US imaging. Successful components of this strategy include the ability to control the size and shape of the ablation so that precise destruction is possible for a small organ like the prostate. This is different compared to the liver, where the size of thermal coagulation is seldom a limiting factor. In addition, the presence of vital structures close to the area of ablation means that the margin of ablation must be known or monitored during ablation. Inadvertent damage to adjacent vital structures will limit the usefulness of this strategy.

In our previous study, we optimized

RF ablation, contrast agent injection, and imaging parameters in contrast-enhanced transrectal US for guiding, monitoring, and controlling thermal ablation of the prostate (13). In our current study, we demonstrate that contrast-enhanced US-guided RF ablation of the entire prostate is technically possible (the average volumes of prostate ablation achieved in the three groups were 96.6%, 91.9%, and 92%, respectively). Although periurethral blood flow serves as a natural heat sink during the ablation and provides partial protection of the urethra, native periurethral flow is inadequate for the preservation of the urethra. Additional cooling protection, by means of infusion of cold saline into the urinary bladder, provides more protection and reduces the likelihood of damage to the urethra from ablation ($P = .002$). Infusion of cold saline via the iliac arteries into the prostate blood vessels did not provide a statistically significant improvement in the protection of the NVB in this small study ($P = .069$).

Cryoablation is a similar procedure to thermal (ie, RF) ablation and has been used clinically for the treatment of prostate cancer (15–17). With this technique, five or six cryoneedles are inserted into the prostate at same time to freeze the gland. Multiple cryoneedles are used simultaneously, because the frozen tissue (ie, the iceball) creates a shadowing artifact that limits visualization of the surrounding tissue. Only the edge of the iceball close to the US transducer can be imaged, which means that the size and extent of the cryoablation area cannot be precisely monitored with US imaging (unlike the results for RF ablation presented here). In a large serial study (17) of 106 patients undergoing percutaneous cryosurgery of prostate cancer, postoperative impotence occurred in 87% of previously potent patients. This could be related to poor control of the extent of the frozen volume and a lack of precise monitoring. Our results suggest that RF ablation with contrast-enhanced US monitoring may not have these limitations.

Although we believe an advantage of our study design is the direct comparison of US with pathologic assessment, several limitations arise from the immediate pathologic sectioning of the prostate gland in our study. It is not known if the thermally damaged urethra and neurovascular tissue would have recovered normal physiologic function. Additional animal studies will be necessary to evaluate the long-term function of the urethra and the NVB. Although we did not measure temperatures in the urethra and the iliac arteries, the more important issue is the pathologic and functional assessment of whether these tissues remain viable. We performed an immediate pathologic evaluation in this study. Future investigations will need to correlate the degree of urethral cooling with follow-up functional viability. We note that in the nonprotected group 1 and the protected groups 2 and 3, the average volume of ablation of the prostate was 96.6% versus 91.9% and 92%, which implies that cooling the urethra and the NVB may increase the heat sink effect throughout the gland and reduce the targeted volume of the ablation. Follow-up studies will be needed to determine whether this results in long-term periurethral tumor recurrence.

The use of a single session for RF ablation of the entire gland simplified our study design, but may limit the utility of the ablation technique. Cooling and heating effects in a single session may temporarily change the microcirculation of the blood supply and limit the detection of viable areas with use of contrast-enhanced US. Therefore, multiple session of RF ablation may be necessary to improve destruction of the entire prostate without damaging the surrounding vital structures.

The major challenge of whole prostate ablation in situ is to protect the surrounding vital structures. Our study demonstrates that contrast-enhanced US with urethral cooling technique allows safe and complete ablation of the prostate in an animal model. The application of intraarterial cooling did not provide a statistically significant improvement in the protection of the NVB in this small study.

**Practical application:** Ideal image guidance during an ablation procedure includes clear delineation of the target and the surrounding anatomy with real-time and multiplanar capabilities. Our study demonstrates a new method of using contrast-enhanced US for precisely guiding and monitoring RF thermal ablation of canine prostate. Contrast-enhanced US imaging can play a key role in guiding RF ablation of the entire prostate. Cold saline infusion provides effective protection of the urethra during thermal ablation. Compared with current techniques, such as brachytherapy, cryoablation, and radical prostatectomy, the predicted advantages of RF thermal ablation of the whole prostate by using contrast-enhanced US guidance will be less invasive with a more precise control of tumor destruction.

## References

1. Lim AJ, Brandon AH, Fiedler J, et al. Quality of life: radical prostatectomy versus radiation therapy for prostate cancer. J Urol 1995;154:1420–1425.
2. Lawton CA, Won M, Pilepitch MV, et al. Long-term treatment sequelae following external bean irradiation for adenocarcinoma of the prostate: analysis of RTOG studies 7506 and 7706. Int J Radiat Oncol Biol Phys 1991;21:935–939.
3. Scardino PT, Frankel JM, Wheeler TM, et al. The prognostic significance of post-irradiation biopsy results in patients with prostatic cancer. J Urol 1986;135:510–516.
4. Gerber GS, Thisted RA, Scardino PT, et al. Results of radical prostatectomy in men with clinically localized prostate cancer. JAMA 1996;276:615–619.
5. Thiel R, Ackermann R. Avoiding complications of radical retropubic prostatectomy. Eur Urol 1997;31:9–15.
6. Trojan L, Kiknavelidze K, Knoll T, Alken P, Michel MS. Prostate cancer therapy: standard management, new options and experimental approaches. Anticancer Res 2005;25(1B):551–561.
7. Blasko JC, Rayde H, Luse RW, et al. Should brachytherapy be considered a therapeutic option in localized prostate cancer? Urol Clin North Am 1996;23:633–650.
8. Long JP, Fallick ML, LaRock DR, Rand W. Preliminary outcomes following crysurgical ablation of the prostate in patients with

clinically localized prostate carcinoma. J Urol 1998;159:477–484.

9. Fournier GR Jr, Narayan P. Laser effects on prostatic tissue: review of experimental data. J Endourol 1995;9:89–92.
10. Madersbacher S, Pedevilla M, Vingers L, Susani M, Marberger M. Effect of high-intensity focused ultrasound on human prostate cancer in vivo. Cancer Res 1995; 55:3346–3351.
11. Devonec M, Ogden C, Perrin P, St Clair Carter S. The clinical response to transurethral microwave thermotherapy is thermal dose dependent. Eur Urol 1993; 23:267–274.
12. Goldberg NS, Dupuy DE. Image-guided radiofrequency tumor ablation. I. Challenges and opportunities. J Vasc Interv Radiol 2001;12:1021–1032.
13. Liu JB, Merton DA, Wansaicheong G, et al. Contrast enhanced US for monitoring radio frequency ablation of canine prostates: initial results. J Urol 2006;176: 1654–1660.
14. Adegboyega PA, Adesokan A, Haque AK, Boor PJ. Sensitivity and specificity of triphenyl tetrazolium chloride in the gross diagnosis of acute myocardial infarcts. Arch Pathol Lab Med 1997;121:1063–1068.
15. Onik GM, Cohen JK, Reyes GD, Rubinsky B, Chang Z, Baust J. Transrectal ultrasound-guided percutaneous radical cryosurgery ablation of the prostate. Cancer 1993;72:1291–1299.
16. Izawa JI, Morganstern N, Chan DM, Levy LB, Scott SM, Pisters LL. Incomplete glandular ablation after salvage cryotherapy for recurrent prostate cancer after radiotherapy. Int J Radiat Oncol Biol Phys 2003; 56(2):468–472.
17. Han KR, Cohen JK, Liller RJ, et al. Treatment of organ confined prostate cancer with third generation cryosurgery: preliminary multi-center experience. J Urol 2003;170:1126–1130.